Correlation between the magnetic irreversibility limit and the zero resistance point in different granular $YBa_2Cu_3O_{7-\delta}$ superconductors

F. T. Dias and V. N. Vieira
Instituto de Física e Matemática, Universidade Federal de Pelotas (UFPEL), Caixa Postal 354, CEP 96010-900, Pelotas, Rio Grande do Sul, Brazil

P. Rodrigues, Jr.
Departamento de Física, Universidade Estadual de Ponta Grossa (UEPG), CEP 84030-000, Ponta Grossa, Paraná, Brazil

X. Obradors
Institut de Ciència de Materials de Barcelona, CSIC, Campus Universitat Autònoma de Barcelona, 08193, Bellaterra, Spain

P. Pureur and J. Schaf*
Instituto de Física, Universidade Federal do Rio Grande do Sul (UFRGS), CEP 91501-970, Porto Alegre, Rio Grande do Sul, Brazil
(Received 1 June 2007; published 2 April 2008)

We report on magnetization and magnetoresistance measurements of single-crystal, melt-processed, and polycrystalline $YBa_2Cu_3O_{7-\delta}$ samples with the purpose of disclosing the connection between the magnetic irreversibility limit and the zero resistance temperature point as a function of applied field in the above samples with very different superconducting granularities. Another goal is to find out how much the applied fields degrade the grain couplings and the electric conductivity for the different field-current configurations. In homogeneous superconductors, the magnetic irreversibility line is well known as a limit below which an electric current different from zero can flow without resistance. Our data for the single crystal with a weak superconducting granularity closely follow this rule. However, the results on the other samples are quite different. Normally, good-quality melt-processed $YBa_2Cu_3O_{7-\delta}$ samples do not exhibit the signature of superconducting granularity. Nevertheless, x-ray analysis of our melt-processed sample, containing 30 wt % of the Y_2BaCuO_5 phase, shows considerable misalignment of the crystallite c axis, which weakens the grain couplings and hence is expected to result in superconducting granularity. Effectively, the magnetic irreversibility lines for $H\|c$ axis as well as for $H\|ab$ plane exhibit, in the low-field region, the usual signature of superconducting granularity. On the other hand, the zero resistance data for increasing fields along the c axis and $J\|ab$ plane split away from the irreversibility line toward the lower-temperature side. Nevertheless, for $H\|J\|ab$ plane, the zero resistance data closely follow the irreversibility line up to the highest applied fields. In the polycrystalline $YBa_2Cu_3O_{7-\delta}$ sample, in which the grain junctions are much weaker, the effect of an increasing applied field on the grain couplings is much stronger. The zero resistance line is already split from the irreversibility line and is lower by more than 17 K at 8 kOe. Our present measurements provide good quantitative data for the discrepancy between the zero resistance and magnetic irreversibility lines. We explain these features in terms of the superconducting glass model.

DOI: 10.1103/PhysRevB.77.134503 PACS number(s): 74.81.Bd, 74.25.Qt

I. INTRODUCTION

It is well established that in homogeneous superconductors the magnetic irreversibility line $T_{irr}(H)$ defines a boundary in the field-temperature (H-T) plane below which the magnetization is irreversible and up to which a nonzero electric current can flow without any resistance. Above this line the magnetization is reversible and all electric transport is resistive due to dissipation by flux dynamic effects. Very clean and well-oxygenated $YBa_2Cu_3O_{7-\delta}$ single crystals are rather homogeneous superconductors.[1] In such single crystals, the electrical resistivity is expected to vanish at the irreversibility line and even to comply with the planar anisotropy of the magnetic irreversibility. However, in general high-temperature superconducting cuprates (HTSCs) are inhomogeneous superconductors.[2,3] Some authors believe that the HTSCs are intrinsically inhomogeneous.[4] In such granular superconductors the magnetic irreversibility and the electrical resistivity do not depend on the same parts of the sample. While the magnetic irreversibility depends on well-coupled grain clusters, the electrical resistance depends on grain arrays traversing the whole sample. Along such long-range paths, zero resistance can be attained only at some temperature below the irreversibility limit.[5] On the other hand, in fields above several kOe, for which the magnetic field penetrates the grains, the magnetic irreversibility is dominated by the intragrain Abrikosov flux dynamics while the electrical resistivity is still ruled by the grain junctions. It can vanish only after long-range coherence is achieved.

Several systematic magnetic irreversibility studies on pure $YBa_2Cu_3O_{7-\delta}$ single crystals, as well as on single crystals doped with Ca, Sr, Zn, or Mg,[1–3] show the signature of superconducting granularity in the low-field region, where the Josephson flux dynamics dominates. Some precise studies of the resistive transition and zero resistance, as a function of low applied fields, also have been made in single crystals[6]

and in polycrystalline samples.[6,7] Although in some cases the data for zero resistance fall below the magnetic irreversibility line, the authors admitted that in high applied fields, where the flux dynamics is dominated by the intragrain Abrikosov flux, the line of zero resistance again follows the irreversibility line.[7–9] The data we are going to disclose here do not corroborate this expectation.

High-quality melt-processed $YBa_2Cu_3O_{7-\delta}$ materials (Y123 phase), having highly aligned *c* axis of the crystallites, normally do not exhibit the signature of superconducting granularity in spite of their polycrystallinity. The linking between the crystallites is so strong that the superconducting grain coupling occurs almost simultaneously with the superconducting transition. Usually these materials exhibit domains with a high density of twinning plains. Pinning, due to such correlated defects in $YBa_2Cu_3O_{7-\delta}$ single crystals[2,10] as well as in melt-processed monodomains,[11] exhibits a strong angular dependence, and hence so do the magnetoresistance and the magnetic irreversibility. Melt-processed materials have also been grown with inclusions of Y_2BaCuO_5 (Y211 phase) particles up to 30 wt %. The interface of the Y211 particles, embedded in the Y123 phase, gives rise to strong isotropic pinning. Several magnetoresistance studies of twinning monodomains, cut from the melt-processed button, have evidenced the strong isotropic pinning effects of the Y211 particles. Besides the strong isotropic pinning, these measurements also revealed the effects of the intrinsic pinning due to the planar superconductivity of the Y123 phase as well as the strongly angular-dependent pinning of the twinning planes.[12–14] Our present study, including a melt-processed sample doped with 30 wt % of Y211 particles and displaying superconducting granularity, will evidence important additional characteristics.

In the present work, we obtain precise profiles of the magnetic irreversibility limit $T_{irr}(H)$ and of the zero resistance point $T_{c0}(H)$ as a function of applied field for three samples of Y123-based superconductors having rather distinct microstructures: (i) a Sr-doped ceramic $YBa_{1.75}Sr_{0.25}Cu_3O_{7-\delta}$ sample (Poly I); (ii) a Zn-doped single crystal $YBa_2Cu_{2.97}Zn_{0.03}O_{7-\delta}$ (SCrZn) and (iii) a melt-processed $YBa_2Cu_3O_{7-\delta}$ sample (Melt-Tex) containing 30 wt % of Y211 phase. Our goal is to disclose the connection between the magnetic irreversibility limit and the zero resistance points in these granular superconductors. As $T_{irr}(H)$ and $T_{c0}(H)$ are measured in the same specimens, this comparison is indeed meaningful. We obtain the magnetic irreversibility from magnetization measurements as a function of temperature, $M(T)$, by using the standard method for measuring the magnetic irreversibility. This method consists in finding precisely the bifurcation of $M(T)$ for zero-field-cooled (ZFC) and subsequent field-cooled (FC) runs. In the single-crystal and polycrystalline samples the irreversibility line could be mapped out without special difficulties. However, in the case of the melt-processed sample, we succeeded only after finding a sample in which the flux jumps were particularly mild in the relevant temperature range. Another delicate point in our program is the calibration of the temperature sensors installed in the different measuring systems. In order to obtain meaningful comparison between magnetic and transport data, the temperature sensors and magnets should be precisely calibrated with respect to each other.

II. SAMPLE PREPARATION AND EXPERIMENTAL TECHNIQUES

Our polycrystalline and single-crystal samples were prepared from highly pure Y_2O_3, $BaCO_3$, $SrCO_3$, CuO, and ZnO powders. In the case of the polycrystalline sample, we mixed the constituents in stoichiometric proportions and used the standard method of reaction in solids. The $YBa_2Cu_{2.97}Zn_{0.03}O_{7-\delta}$ single crystals were grown by the usual self-flux method from an initial mix with the proportions of 1:4:9.9:0.1 of Y, Ba, Cu, and Zn, respectively, and oxygenated during ten days at 450 °C. X-ray diffraction on the single crystal used in the measurements revealed a very clean orthorhombic phase, with lattice parameters in agreement with those reported in the literature for the corresponding Zn concentration.[15] Examination of this single crystal with polarized light microscopy showed twinned domains. The polycrystalline $YBa_{1.75}Sr_{0.25}Cu_3O_{7-\delta}$ sample (Poly-I) for magnetic measurements was a slender double-wedge-shaped specimen of nearly 1 cm long, while that for the resistivity measurements was a long parallelepiped 10 mm long and of 1 mm^2 cross section. The $YBa_2Cu_{2.97}Zn_{0.03}O_{7-\delta}$ single crystal (SCrZn) was a long rectangular platelet of close to 2 mm^2 in area and of about 0.12 mm in thickness. The same specimen was used in the magnetic and transport measurements. Our melt-processed $YBa_2Cu_3O_{7-\delta}$ sample (Y123 phase), containing 30 wt % of Y_2BaCuO_5 (Y211 phase) and 1 wt % of CeO_2, was prepared by the top-seeding method. Initially a pellet with a total mass of about 5 g consisting of well-mixed Y123, Y211, and CeO_2 was sintered at 920 °C during 24 h. Then, after placing a $NdBa_2Cu_3O_{7-\delta}$ single crystal on top of the pellet, the melt-texturing temperature cycle described in Ref. 26 was applied. The purpose of the Y211 phase is to introduce a large number of pinning centers. The CeO_2, besides physically stabilizing the melt at high temperatures, limits the size of the Y211 particles, thereby improving the distribution of the Y211 phase. This procedure enhances strongly the flux pinning potential in the melt-processed Y123. A sample (Melt-Tex) for magnetic and electrical transport measurements was cut from the melt-processed button and oxygenated at 420 °C under pure flowing oxygen for 5 days. The Melt-Tex sample was a long parallelepiped 8 mm in length along the *ab* plane, 1.3 mm along the *c* axis, and 1.3 mm in thickness (*ab* plane).

The dc magnetization measurements were made using a superconducting quantum interference device (SQUID) MPMS-XL magnetometer from Quantum Design. The method consisted in first cooling down the sample to temperatures well below T_c in zero field (ZFC). Then the magnetization $[M_{ZFC}(T)]$ was measured under constant magnetic field while slowly warming the sample (0.2 K/min or less) up to temperatures well above T_c. Fields within the range 3–50 kOe were applied. Subsequently the magnetization $[M_{ZFC}(T)]$ was measured while cooling the sample back to temperatures well below T_c in the same field (FC). The irreversibility limit $T_{irr}(H)$ for a given field is the temperature value where the difference $\Delta M(T)=M_{FC}(T)-M_{ZFC}(T)$ deviates from the zero baseline defined by the high-temperature data, where the magnetization is reversible. The M_{FC} and M_{ZFC} data normally show a small temperature gradient of

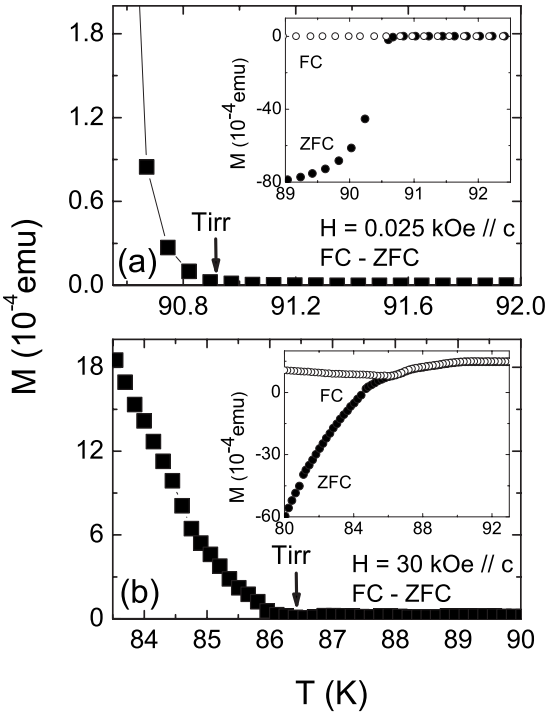

FIG. 1. Two examples of the $\Delta M(T)=M_{FC}(T)-M_{ZFC}(T)$ (main figure) and the $M_{ZFC}(T)$ and $M_{FC}(T)$ magnetization data (inset). The vertical arrows indicate the irreversibility limits $T_{irr}(H)$.

less than 0.1°, which appears as a constant or a linear temperature-dependent term in the $\Delta M(T)$ results. Our data were corrected for temperature gradient effects. The irreversibility limit of the melt-processed sample was also determined from hysteresis cycles up to 1 T. These data were found to be in perfect agreement with those obtained from the $\Delta M(T)$ data.

The magnetoresistance measurements were made in constant applied fields up to 50 kOe using the four-contact method. We used a low-current low-frequency ac technique in which a lock-in amplifier was employed as a null detector. Good electrical contacts were achieved by heating the samples with freshly painted silver paint stripes to 400 °C in pure oxygen for 1 h. The measurements were performed while the temperature was swept (down) very slowly (0.05 K/min) and measured with a Pt thermometer corrected for magnetoresistance effects within a resolution of 0.002 K. The magnetoresistance points were closely spaced so as to allow for a numerical calculation of the temperature derivative of the resistivity, $d\rho(T)/dT$.

III. EXPERIMENTAL RESULTS

A. Magnetic irreversibility

We have determined the magnetic irreversibility limit of our samples for many applied magnetic fields ranging from 3 Oe to 50 kOe. Figure 1 displays two representative examples for the difference $\Delta M(T)=M_{FC}(T)-M_{ZFC}(T)$, chosen among the more difficult measurements for the melt-processed sample (Melt-Tex), in order to illustrate our data analysis. In

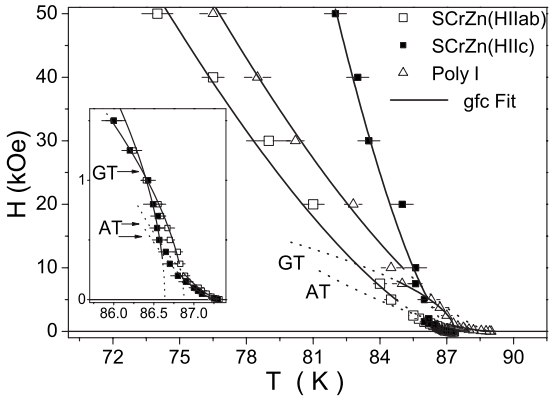

FIG. 2. Irreversibility data for the SCrZn sample for $H\|c$ and $H\|ab$, and for the Poly-I sample. The continuous lines labeled GFC are fittings to the power law predicted by the giant-flux-creep theory [Eq. (1)], while in low fields and in the inset denoted by AT and GT are fittings to the de Almeida–Thouless and Gabay-Toulouse power laws, respectively.

the case of the single crystal and the melt-processed samples we have determined $T_{irr}(H)$ for fields applied along the c axis as well as along the ab plane. The irreversibility limit $T_{irr}(H)$ for the single crystal (SCrZn) and the polycrystalline sample (Poly-I) could be determined with good precision. Figure 2 displays the $T_{irr}(H)$ data of the single crystal for $H\|c$ or $H\|ab$, and for the Poly-I sample for $H\perp J$. The inset highlights the low-field data for the single crystal only. Those of the Poly-I sample are already clear in the main figure.

In the case of the melt-processed sample (Melt-Tex), good irreversibility data could be obtained only after finding a sample where the noise due to flux jumps was low, especially near the irreversibility limit. The very good signal-to-noise ratio of this sample was of much help. Figure 3 displays the irreversibility data of the Melt-Tex sample for $H\|c$ axis and $H\|ab$ plane. The inset highlights the low-field data, where two characteristic regimes are observed.

The continuous lines through the data in the high-field region in Figs. 2 and 3 are fittings with the power law pre-

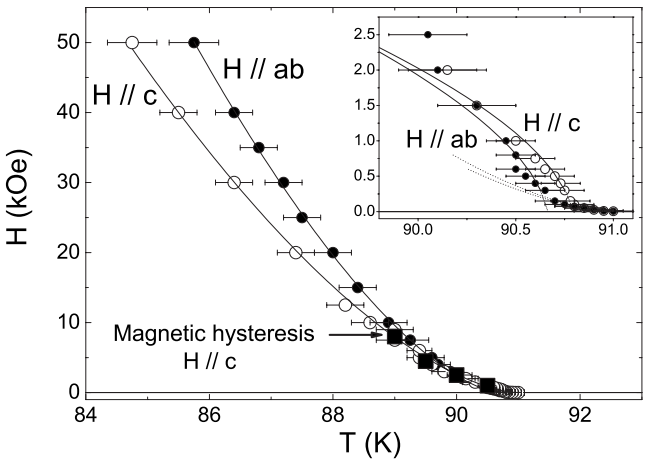

FIG. 3. Same as in Fig. 2 but for the Melt-Tex sample. The large squares are the irreversibility limits from hysteresis loops.

TABLE I. Fitting parameters for the $YBa_2Cu_{2.97}Zn_{0.03}O_{7-\delta}$ single crystal (SCrZn), melt-textured $YBa_2Cu_3O_{7-\delta}$ with 30 wt % Y211 phase inclusions, and the $YBa_{1.75}Sr_{0.25}Cu_3O_{7-\delta}$ (Poly I) polycrystalline sample for $H \| J$.

Sample	Fit	α	H_0 (kOe)	$T_{irr}(0)$ (K)
SCrZn	GFC	1.45 ± 0.16	807.0	87.35
($H \| c$)	GT	0.60 ± 0.09	23.1	86.88
	AT	1.60 ± 0.12	934.1	87.35
SCrZn	GFC	1.60 ± 0.18	873.6	87.30
($H \| ab$)	GT	0.54 ± 0.14	23.9	86.54
	AT	1.60 ± 0.21	1269.5	87.00
Melt-Tex	GFC	1.60 ± 0.12	3574.5	91.00
($H \| c$)	GT	0.58 ± 0.10	33.4	90.78
	AT	1.59 ± 0.16	1442.4	91.00
Melt-Tex	GFC	1.54 ± 0.04	4538.5	90.70
($H \| ab$)	GT	0.60 ± 0.14	37.0	90.65
	AT	1.60 ± 0.27	1285.0	90.90
Poly I	GFC	1.43 ± 0.19	864.2	89.00
	GT	0.55 ± 0.05	54.6	87.37
	AT	1.55 ± 0.13	421.1	89.00

dicted for the irreversibility line by the giant-flux-creep (GFC) theory:[16]

$$H_{irr}(T) = H_0(1-t)^{\alpha} \quad \left(\alpha = \frac{3}{2}\right). \tag{1}$$

In Eq. (1) $t = T_{irr}(H)/T_{irr}(0)$ is the reduced temperature, and H_0 and $T_{irr}(H)$ are fitting parameters. The continuous lines through the low-field data (see insets of Figs. 2 and 3) are fittings with de Almeida–Thouless–like[17] (AT) [$\alpha = 3/2$ in Eq. (1)] and the Gabay-Toulouse-like[18] (GT) [$\alpha = 1/2$ in Eq. (1)] power laws. Although the AT power law has the same form as that of the giant flux creep, its physical background and the fitting parameters are quite distinct. The AT as well as the GT power laws proceed from mean field calculations for the frustrated Ising-like and Heisenberg or *XY* spin-glass systems, respectively. They have extensively been used to describe the irreversibility data of granular superconductors.[1–3,6,7,19] This is no surprise since the grain coupling in grain aggregates of disordered granular superconductors under applied magnetic field is well known to be dominated by frustration, in analogy to the spin coupling in spin-glass systems. Hence the observation of AT and GT power law behavior of the irreversibility line of our granular superconductors shows that they are frustrated superconducting grain aggregates. Table I lists the fitting parameters H_0 and $T_{irr}(H)$ for our samples, corresponding to the giant-flux-creep, the AT-like, and the GT-like power law regimes, respectively.

The $T_{irr}(H)$ data of the Melt-Tex sample for $H \| c$ axis and $H \| ab$ plane in Fig. 3 show a strongly reduced planar anisotropy. This is due to some misalignment of the *c* axis of the crystallites in our melt-processed sample, caused by the high concentration of the Y211 phase.[20] This disorder prevents the Abrikosov flux from being accommodated along the *ab* planes, resulting in considerable loss of the intrinsic pinning and hence loss of the planar anisotropy. Therefore the true magnetic irreversibility for $H \| ab$ is experimentally inaccessible. The large squares in Fig. 3 are the irreversibility limits obtained from hysteresis cycles for fields up to 10 kOe applied along the *c* axis. They are in good agreement with those obtained from the temperature cycles.

Normally melt-processed materials do not display superconducting granularity. However, the high concentration of Y211 phase causes considerable misalignment of the *c* axis, thereby encumbering grain coupling. The effects of granularity in fact are very faint, but thanks to the high precision of the data (see insert in Fig. 3), we can clearly distinguish the AT and GT power law regimes in the low-field region, which are typical of frustrated systems. These low-field data even display the inverted planar anisotropy usually observed in the low-field region of single crystals with a granular superconducting character (see inset in Fig. 2).[2,3] This reversed anisotropy is usually ascribed to the fact that the weak links along the *ab* plane become stable at higher temperatures than along the *c* axis.

B. Magnetoresistivity

We have measured the resistive transition of our Zn-doped $YBa_2Cu_{2.97}Zn_{0.03}O_{7-\delta}$ single crystal for a low measuring current along the *ab* plane and a number of applied magnetic field values (see figure caption) applied along the *c* axis as well as along the *ab* plane. We estimate the excess conductivity $\Delta\sigma$ by subtracting the actually measured conductivity $\sigma(T) = 1/\rho(T)$ from the fitted and extrapolated normal conductivity $\sigma_N(T)$, obtaining $\Delta\sigma(T) = \sigma_N(T) - \sigma(T)$. Assuming that in the immediate vicinity of zero resistance the excess electric conductivity $\Delta\sigma(T)$ diverges according to the power law

$$\Delta\sigma(T) = A\left(\frac{T - T_{c_0}}{T_{c_0}}\right)^{-\lambda}, \tag{2}$$

where *A* is a constant amplitude, T_{c0} is the characteristic transition temperature, and λ is the critical exponent for the coherence transition.[3,5–7,15,21–23] From the experimental data we determine numerically the quantity $\chi_\sigma(T) = -d(\ln \Delta\sigma)/dT$, and obtain

$$\chi_\sigma^{-1}(T) = \frac{1}{\lambda}(T - T_{c0}). \tag{3}$$

Figures 4 and 5 display the $\chi_\sigma^{-1}(T)$ curves for several magnetic fields applied along the *c* axis and parallel to the *ab* plane, respectively. The straight lines are fittings to Eq. (3). Within our experimental precision, the exponents, obtained from the slope of these fittings, are in agreement with the theoretically expected values for the coherence transition.[5,15,21–23] On the other hand, we determine the temperature points where the resistivity falls to zero by extrapolating the power law regimes to the temperature axis. In Figs. 4 and 5 we also mark the irreversibility limits on the fittings to $\chi_\sigma^{-1}(T)$ for each applied magnetic field. We can clearly

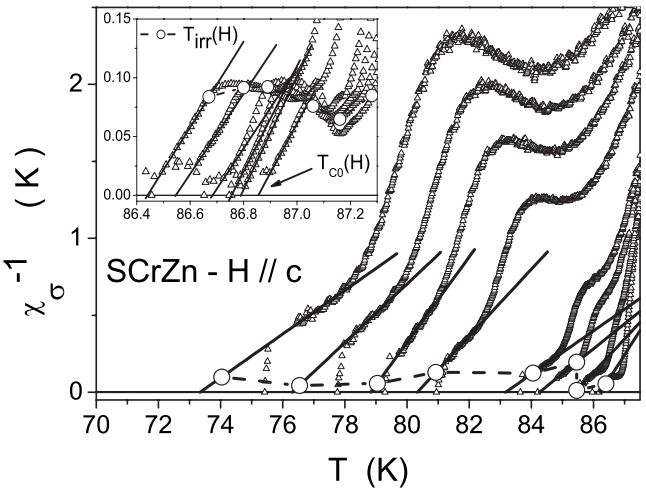

FIG. 4. $\chi_\sigma(T)^{-1}$ data for the single crystal (SCrZn) in fields (from right to left) $H=1$, 2.5, 5, 7.5, 20, 30, 40, and 50 kOe, applied along the c axis. The inset shows data for $H=0.01$, 0.05, 0.1, 0.2, 0.4, and 0.6 kOe. The measuring current is applied parallel to the ab plane. Straight lines are fittings with the power law Eq. (3). The exponents obtained from the fittings range from the theoretically predicted value (4) up to 40 kOe. The open circles represent the positions of the irreversibility limit for the respective applied fields.

observe that, within our experimental precision, the magnetic irreversibility points and the zero resistance points are closely together in the high-field region. However, in low fields where our experimental precision is higher (see inset in Figs. 4 and 5 as well as in Fig. 8 of the next section) the zero resistance points fall systematically below the irreversibility line. In the next section, we discuss in detail the correlation between the magnetic irreversibility and the zero resistance points. Figure 6 displays analogous results for the polycrystalline sample Poly-I (see field values in the caption). In this case, the zero resistance points fall well below the irreversibility line for the whole range of applied fields. The separation between the two characteristic temperatures strongly increases as the value of the applied field is increased. However, in fields higher than 7.5 kOe, the $\chi_\sigma^{-1}(T)$ curves become rounded and no power law regimes can be found.

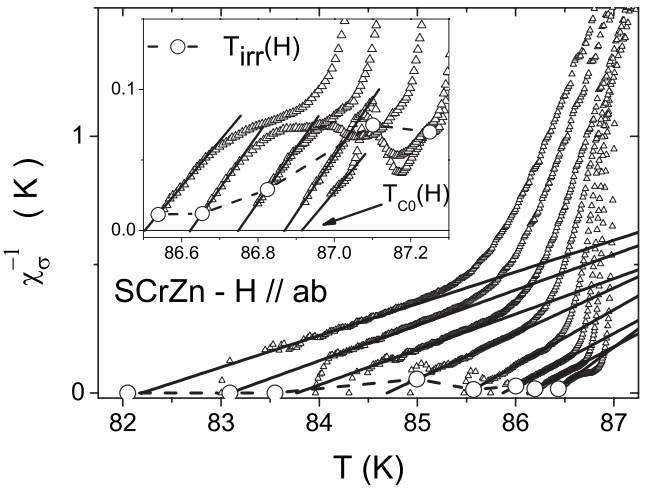

FIG. 5. Same as Fig. 4, for the same fields applied parallel to the ab plane (absent is 0.05 kOe and included is 10 kOe).

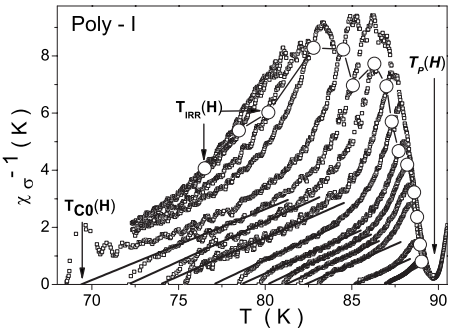

FIG. 6. Same as Figs. 4 and 5, but for the Poly-I sample and magnetic fields of $H=0.002$, 0.01, 0.05, 0.1, 0.2, 0.4, 1, 2.5, 5, 7.5, 10, 20, 30, 40, and 50 kOe applied parallel to the measuring current. $T_P(H)$ is the temperature point where the temperature derivative of the resistivity is maximum.

It may be noted in Figs. 4 and 5 that in the vicinity of zero resistance the $\chi_\sigma^{-1}(T)$ data for the highest magnetic fields close to the zero resistance state do not follow the power law regime, but fall abruptly to zero before the power law regime reaches the temperature axis. This effect is a clear manifestation of the Abrikosov vortex lattice solidification.[24] We should then admit that effects resulting from the Abrikosov vortex dynamics are coexisting with effects specifically related to granularity, which are responsible for the power law behavior of the resistivity in the regime close to the zero resistance state, and for the magnetic irreversibility limit in low fields, which behaves according to the de Almeida–Thouless and Gabay-Toulouse power laws.

The Melt-Tex sample employed in the magnetoresistance measurements was the same one used in the magnetic measurements. The magnetoresistance experiments were performed by applying a low measuring current density ($J=150$ mA/cm^2) parallel to the ab plane and fields along the c axis or alternatively fields along the ab plane and parallel to the current J. We obtained a high density of data points while slowly cooling the sample through the superconducting transition region under constant applied magnetic fields. Figures 7(a) and 7(b) display the magnetoresistivity data under the indicated fields applied along, respectively, the ab plane ($H\|J$) and the c axis. The resistivity is considerably anisotropic for fields along the ab plane or along the c axis. The inset of Fig. 7(a) exemplifies the method used to define the point of zero resistance, since in this sample the quantity $\chi_\sigma^{-1}(T)$ does not show a power law behavior near the zero resistance state. We evaluate the zero resistance temperature by adopting a practical criterion, according to which this temperature is obtained from the threshold of the plateau where $d\rho(T)/dT$ falls to zero. The vertical arrows in the inset indicate the point where the resistance becomes zero according to our criterion. This point is denoted as $T_{R=0}(H)$, for the sake of distinguishing it from $T_{c0}(H)$, obtained from power law regimes. It may be observed that the melt-processed $YBa_2Cu_3O_{7-\delta}$ is much less sensitive to the applied field than the ceramic material.

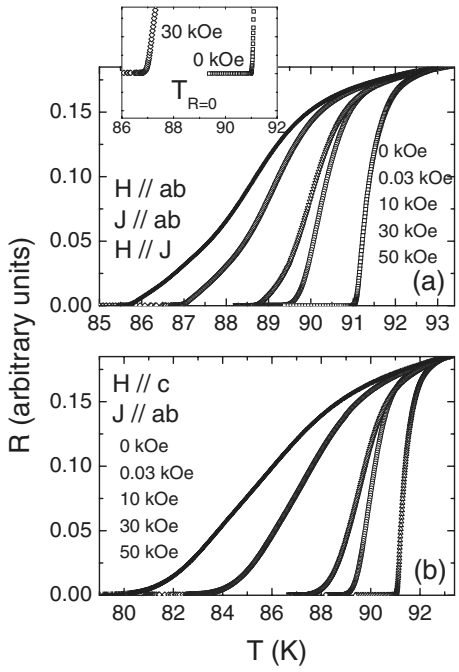

FIG. 7. Resistive transition for the Melt-Tex sample with measuring current in the *ab* plane and fields of the indicated values applied (a) parallel to the *ab* plane and (b) along the *c* axis. The inset exemplifies our method of finding the point of zero resistance $T_{R=0}(H)$ in this case. Note the large anisotropy of $\rho(T)$ with respect to the field orientation.

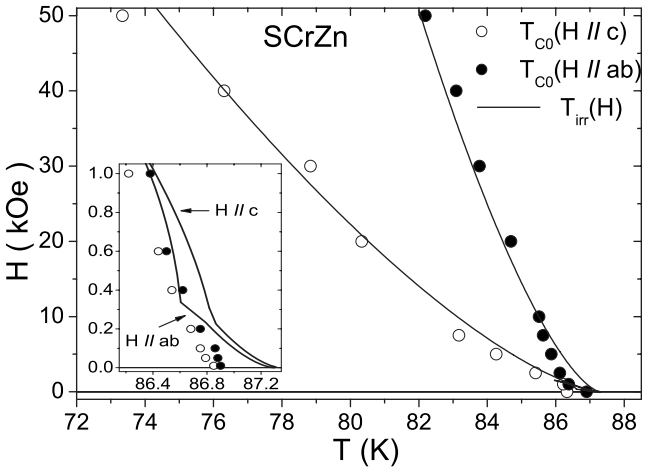

FIG. 8. Irreversibility lines of the SCrZn sample, as fitted in Fig. 2, together with the zero resistance data T_{c0}. The closed circles are for fields applied parallel to the *ab* plane and the open circles are for fields along the *c* axis. The experimental error in T_{c0} is roughly the size of the circles. The inset highlights the data in low fields.

IV. CORRELATION BETWEEN ZERO RESISTIVITY AND MAGNETIC IRREVERSIBILITY

The usual idea that the irreversibility line is a boundary below which an electric current may flow without resistance stems from the conventional homogeneous metallic superconductors. The high-T_c superconducting cuprates normally are granular superconductors in which the onset of magnetic irreversibility takes place as soon as the first loops of coupled grains form. These grain clusters trap Josephson flux and lead to irreversible flux mobility. Nevertheless, under these same circumstances the electric transport still remains resistive because the well-coupled grain clusters, responsible for the magnetic irreversibility, still remain disconnected from each other. The resistivity vanishes only when the grain coupling strength overcomes the phase entropy and leads to long-range coherence of the order parameter. The electrical resistance in granular superconductors is expected to persist down to temperatures below the irreversibility line and to vanish only after the phase coherence percolates through the whole sample.

In order to disclose the correlation between magnetic irreversibility and the zero resistance data of our studied samples, we plot the irreversibility lines $T_{\rm irr}(H)$ together with the corresponding zero resistance $T_{c0}(H)$ data in the same figure. Figure 8 displays the irreversibility lines $T_{\rm irr}(H)$, as fitted to the data of the single crystal (SCrZn) in Fig. 2, together with the corresponding zero resistance data, $T_{c0}(H)$. We have pointed out in Sec. III A that the $T_{\rm irr}(H)$ data of the Zn-doped $YBa_2Cu_3O_{7-\delta}$ single crystal display only a weak superconducting granularity. Therefore the zero resistance data are expected to fall closely below the irreversibility line. Effectively, while in high fields the $T_{c0}(H)$ data fall, within our experimental precision, about the irreversibility line, in the low-field region, where the experimental precision is better, they fall systematically underneath the irreversibility line for both field directions (see inset in Fig. 8).

High-quality melt-processed $YBa_2Cu_3O_{7-\delta}$ materials containing less than 25 wt % of the Y211 phase, usually exhibit no superconducting granularity.[12,25] Nevertheless, higher concentrations of the Y211 phase are known to cause misalignment of the *c* axis, reducing the planar anisotropy.[20,25] Our sample contains 30 wt % of the Y211 phase and exhibits a relevant superconducting granularity. This granularity is evidenced[1–3] by the presence of the AT and GT power law regimes in the low-field irreversibility data (see inset in Fig. 3). This granularity arises mainly from misalignment of the *c* axis. Although the $\chi_\sigma^{-1}(T)$ curves of this sample disclose a characteristic hump below the pairing transition, due to grain coupling and the coherence transition, we were not able to identify power law regimes there. Apparently the coherence transition takes place too close to the superconducting transition so that it is buried by it.

Figure 9 displays the irreversibility lines of the melt-processed sample, as obtained from fittings to the irreversibility data in Fig. 3 for both applied field directions, together with the corresponding zero resistance data, $T_{R=0}(H)$. Note that, in our measurements, the measuring current flows along the same *ab* planes for both field orientations. While for $H\|ab$ plane and $H\|J$ the zero resistance data (closed circles) fall closely underneath the corresponding irreversibility line, for $H\|c$ axis and $H\perp J$ (open circles) they split strongly away from the irreversibility line toward lower temperatures. Our melt-processed sample is a relatively large parallelepiped, not a twinning monodomain, and so the twinning domains must be nearly random in the *ab* plane. Their direction also must be scattered somewhat about the average *c* axis,

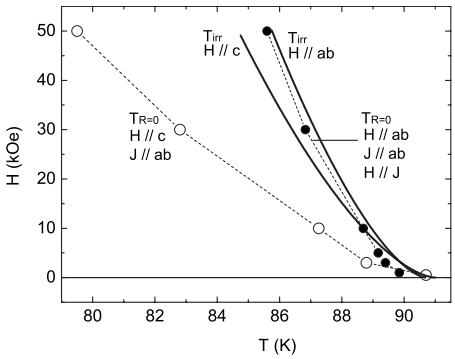

FIG. 9. Same as Fig. 8 but for the Melt-Tex sample.

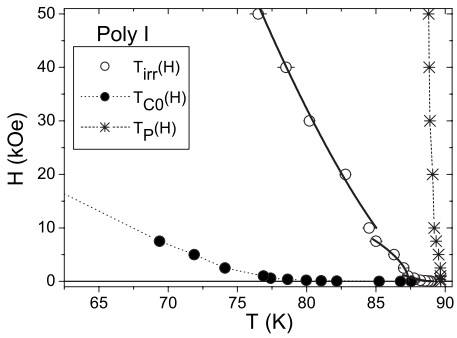

FIG. 10. Same as Figs. 8 and 9, but for the Poly-I sample. Open circles are the irreversibility data and closed circles are zero resistance data. The asterisks indicate the approximate superconducting transition temperatures.

due to the noncollinearity of the crystallite c axes. Therefore, while flux pinning by the twinning planes certainly contributes somewhat for fields applied along the c axis, its contribution for fields along the ab plane must be irrelevant. It also is observed that the irreversibility data disclose a much reduced c -axis ab -plane anisotropy. This is due to the spreading out of the c axes of the different crystallites and the consequent noncoplanarity of the ab planes. The irreversibility and magnetoresistance data also certainly comprise the effects of the strong isotropic pinning of the Y211 inclusions.[12] However, besides all these contributions to the pinning, the magnetoresistance and magnetic irreversibility data of our melt-processed sample also discloses the effects induced by the applied field on the grain coupling. In this sense our data complement the data of Ref. 12. The origin of these granularity effects will be discussed in detail in the next section.

Our polycrystalline sample exhibits a strong superconducting granularity, as is shown by the very clear presence of the AT and GT regimes in the low-field irreversibility data. The magnetoresistance data, displayed in Fig. 6, also disclose a clear grain coupling process. Therefore the zero resistance points $T_{c0}(H)$ could be found by extrapolating the power law regimes in the $\chi_\sigma^{-1}(T)$ curves to the temperature axis. In spite of the field being applied parallel to the measuring current, $H \| J$, the zero resistance data of this sample fall considerably below the irreversibility line already in low fields and split away from this line very steeply when the applied field increases. These data fall already 17 K below the irreversibility line when the field attains $H=8$ kOe (see Fig. 10). In polycrystalline samples the flow of the measuring current through the grain aggregate is highly dispersive and therefore $H \| J$ is microscopically only a rudimentary approximation. For $H \perp J$ we would expect a much more drastic effect of an applied field on the resistivity. Our data also show no indication that the zero resistance data might come back and meet the irreversibility line somewhere in higher fields.

V. DISCUSSION

A magnetic field applied to a granular superconductor is well known to increase the phase entropy.[26] The field, while randomly distorting the phase of the order parameter, weakens and frustrates the grain coupling and favors the phase fluctuations that result in the increase of the magnetoresistance. These random phase distortions also weaken the ability of the grain aggregate to pin the intergrain Josephson flux that dominates in the low-field region. Therefore, in this region the magnetic irreversibility line exhibits the AT- and GT-like power laws that are the signature of frustrated systems. The zero resistance temperature point is particularly sensitive to the direction of the applied field with respect to the current flow.[27] The effect of an applied field for the different orientations with respect to the crystal axes and with respect to the measuring current may be highlighted by careful analysis of our zero resistance and magnetic irreversibility data for the different field-current configurations.

The response of a granular superconductor to an applied magnetic field usually is described in terms of the effective Josephson coupling Hamiltonian:[26]

$$H = -\sum_{i,j} J_{ij} \cos(\theta_i - \theta_j - A_{ij}). \tag{4}$$

Here J_{ij} are the phase coupling energies between neighboring grains i and j and $\theta_i - \theta_j$ is the phase difference of the Ginsburg-Landau order parameter on the grains i and j. The phase displacements A_{ij}, caused by the applied magnetic field, are given by

$$A_{ij} = \frac{2\pi}{\phi_0} \int_i^j \vec{A} \cdot \vec{dl}, \tag{5}$$

where ϕ_0 is the elementary flux quantum, $\vec{A}$ is the vector potential along the weak link between grains i and j, and the line integral is evaluated between the centers of grains i and j. Equation (5) shows that an applied field causes phase displacements of the GL order parameter along those weak links which extend along the vector potential $\vec{A}$. In other words, the A_{ij} are large along weak links that lie transversely to the applied magnetic field but may vanish along the weak links oriented parallel to the applied field.

Due to the dependence of the phase displacements A_{ij} and the associated grain decoupling effect on the direction of the applied field with respect to the weak links, the magnetic

irreversibility and the zero resistance limit of granular superconductors depend strongly on the field-current configuration. If, for instance, the field is applied along the *c* axis and the measuring current flows in the *ab* plane, the degradation of the conducting junctions is expected to be strong, leading to a considerable increase of the resistivity and a large displacement of the zero resistance point to lower temperatures. This is corroborated by the large displacement of the zero resistance limit to lower temperatures with respect to the locus of the irreversibility line in the data plotted in Fig. 9 and also agrees with the results of $\rho(T)$ for a Ca-doped single crystal,[27] which undergoes a considerable displacement for $H\|c$ axis and $J\|ab$ plane. If, however, the field direction is parallel to the measuring current in the *ab* plane, the effect of the field on the weak links carrying the current is expected to be much smaller. This is what is seen in Fig. 9 and also is corroborated by the data on the Ca-doped single crystal[27] where the resistivity undergoes only an irrelevant displacement for $H\|J$.

In the case of the polycrystalline sample (Poly-I), in which the links between the grains are much weaker, the effects of the applied field on the grain coupling is very drastic even for fields applied parallel to the intended measuring current. Obviously, in granular superconductors the direction of the measuring current is microscopically disperse because of the complicated coupled grain arrays that percolate through the sample in complicated loops. When $H \perp J$ the decoupling effect of the applied field may even be much stronger.

VI. CONCLUSIONS

Our experimental results show clearly that the zero resistance in granular superconductors is inexorably ruled by grain couplings. These results also show that the effect of an applied field on the resistivity depends strongly on the field-current configuration. In single crystals, having a weak superconducting granularity, the electrical resistance vanishes very close to and underneath the magnetic irreversibility line, especially when the applied field lies parallel to the measuring current. However, in the case of samples with a strong superconducting granularity, our data show that an applied magnetic field severely degrades the grain couplings extending transversally to the applied field, that is, lying along the vector potential of the field. The electrical resistance, for current flowing along the weak links affected by the applied field, vanishes only far below the irreversibility line. Nevertheless, the weak links lying parallel to the applied field are much less affected. Our data also strongly exclude the possibility of the zero resistance and the magnetic irreversibility data of granular superconductors coming back and meeting together somewhere in high fields.

ACKNOWLEDGMENTS

The authors thank the Brazilian agencies CNPq and FAPERGS for partially financing this work.

*Corresponding author. FAX: (55) (51) 3308 7286. schaf@if.ufrgs.br

[1] V. N. Vieira, J. P. da Silva, and J. Schaf, Phys. Rev. B **64**, 094516 (2001).
[2] V. N. Vieira and J. Schaf, Phys. Rev. B **65**, 144531 (2002).
[3] V. N. Vieira, P. Pureur, and J. Schaf, Phys. Rev. B **66**, 224506 (2002).
[4] E. Dagotto, Science **309**, 257 (2005).
[5] J. Rosenblatt, P. Peyral, A. Raboutou, and C. Lebeau, Physica B **152**, 95 (1988).
[6] V. N. Vieira, P. Pureur, and J. Schaf, Physica C **354**, 299 (2001).
[7] J. Roa-Rojas, R. Menegotto Costa, P. Pureur, and P. Prieto, Phys. Rev. B **61**, 12457 (2000).
[8] F. W. Fabris, J. Roa-Rojas, and P. Pureur, Physica C **354**, 304 (2001).
[9] F. W. Fabris, Ph.D. thesis, Instituto de Física, UFRGS, RS, Brazil, 2005, p. 105.
[10] S. Fleshler, Wai-Kwong Kwok U. Welp, V. M. Vinokur, M. K. Smith, J. Downey, and G. W. Crabtree, Phys. Rev. B **47**, 14448 (1993).
[11] S. Sanfilippo, A. Sulpice, O. Laborde, D. Bourgault, Th. Fournier, and R. Tournier, Phys. Rev. B **58**, 15189 (1998).
[12] J. Figueras, T. Puig, and X. Obradors, Phys. Rev. B **67**, 014503 (2003).
[13] T. Puig, F. Galante, E.M. Gonzalez, J.L. Vicent, B. Martinez, and X. Obradors, Phys. Rev. B **60**, 13099 (1999).
[14] J. Figueras, T. Puig, X. Obradors, W. K. Kwok, L. Paulius, G. W. Crabtree, and G. Deutscher, Nat. Phys. **2**, 402 (2006).
[15] C. Y. Yang, A. R. Moodenbaugh, Y. L. Wang, Y. Xu, S. M. Heald, D. O. Welch, M. Suenaga, D. A. Fischer, and J. E. Penner-Hahn, Phys. Rev. B **42**, 2231 (1990).
[16] Y. Yeshurun and A. P. Malozemoff, Phys. Rev. Lett. **60**, 2202 (1988).
[17] J. R. L. de Almeida and D. J. Thouless, J. Phys. A **11**, 983 (1978).
[18] M. Gabay and G. Toulouse, Phys. Rev. Lett. **47**, 201 (1981).
[19] M. Suzuki, I. S. Suzuki, and J. Walter, Physica C **402**, 243 (2004).
[20] A. E. Carrillo, T. Puig, J. Plain, J. Figueras, and X. Obradors, Physica C **336**, 213 (2000).
[21] A. R. Jurelo, J. V. Kunzler, J. Schaf, P. Pureur, and J. Rosenblatt, Phys. Rev. B **56**, 14815 (1997).
[22] R. M. Costa, P. Pureur, M. Gusmao, S. Senoussi, and K. Behnia, Phys. Rev. B **64**, 214513 (2001); see also R. M. Costa, P. Pureur, M. Gusmao, S. Senoussi, and K. Behnia, Solid State Commun. **113**, 23 (1999).
[23] P. Pureur, R. Menegotto Costa, P. Rodrigues, Jr., J. Schaf, and J. V. Kunzler, Phys. Rev. B **47**, 11420 (1993).
[24] H. Safar, P. L. Gammel, D. A. Huse, D. J. Bishop, J. P. Rice, and D. M. Ginsberg, Phys. Rev. Lett. **69**, 824 (1992).
[25] F. T. Dias, Ph.D. thesis, Instituto de Física, UFRGS, RS, Brazil, 2003, p. 188.
[26] W. Y. Shih, C. Ebner, and D. Stroud, Phys. Rev. B **30**, 134 (1984).
[27] V. N. Vieira, I. C. Riegel, and J. Schaf, Phys. Rev. B **76**, 024518 (2007).